Subcellular localization of the chemotherapeutic agent doxorubicin in renal epithelial cells and in tumor cells using correlative light and electron microscopy

Claudia Asam[a], Korbinian Buerger[a], Oliver Felthaus[c], Vanessa Brébant[c],
Reinhard Rachel[b], Lukas Prantl[c], Ralph Witzgall[a], Silke Haerteis[a,*] and Thiha Aung[c]

[a]*Institute for Molecular and Cellular Anatomy, University of Regensburg, Germany*
[b]*Centre for Electron Microscopy, Faculty of Biology and Preclinical Medicine,
University of Regensburg, Germany*
[c]*Centre of Plastic, Aesthetic, Hand and Reconstructive Surgery, University of Regensburg,
Regensburg, Germany*

Abstract.
BACKGROUND: Doxorubicin is a cytostatic drug from the group of anthracycline antibiotics that is widely used as a chemotherapeutic agent. Side effects of the active substance include cardiotoxicity and nephrotoxicity. Doxorubicin-treated renal epithelial cells and (sarcoma) tumors are examined by correlative light and electron microscopy (CLEM) to investigate the subcellular localization of doxorubicin.
METHODS: The kidney epithelial cell line MDCK II (Madin-Darby Canine Kidney) grown on culture dishes were treated with doxorubicin. Subsequently, the cells are analyzed by means of fluorescence and transmission electron microscopy (TEM). *In vivo*, alveolar rhabdomyosarcoma (RH 30) tumor cells are transferred to the chorioallantoic membrane (CAM) of the chicken embryo. Doxorubicin is injected into a vein of the chicken embryo. After 24 hours, the tumor is removed and examined using CLEM.
RESULTS: The kidney epithelial cells and the doxorubicin-injected tumors show a clear staining of the cell nucleus, which correlates with electron-dense regions (heterochromatin). High-resolution TEM shows that doxorubicin treatment leads to an enormous stress situation with an increased formation of membrane blebbings.
CONCLUSIONS: CLEM is a promising new method to visualize the pattern of fluorescing drugs (e.g. doxorubicin) in renal epithelial cells and tumors, and to localize the drug in its subcellular context combined with high resolution.

Keywords: Correlative light and electron microscopy (CLEM), chorioallantoic membrane (CAM), doxorubicin, chemotherapy, tumor, sarcoma, Epon

1. Introduction

Since pioneers of microscopy like Antoni van Leeuwenhoek started investigating biological structures in the 17th century, the angular resolution has been restricted by the diffraction limit of visible light. Nowadays super-resolution techniques have achieved resolutions below 50 nm down to a macromolecular level [1–3]. Super-resolution methods are based either on exploitation of shaped illumination beams or utilize stochastic or photoactivated switching of fluorophores. Various super-resolution techniques have been developed. (i) Single molecule localization microscopy (SMLM) uses photoswitchable

*Corresponding author: Silke Haerteis, Institute for Molecular and Cellular Anatomy, University of Regensburg, Universitätsstr. 31, 93053 Regensburg, Germany. E-mail: silke.haerteis@ur.de.

fluorescent probes. Isolated emitters are repeatedly localized and a super-resolution image is built from these single-molecule localizations [4]. (ii) Structured illumination microscopy (SIM) is a widefield microscopy technique that uses the Moiré effect to double the spatial resolution [5]. (iii) In stimulated emission depletion (STED) microscopy, fluorophores are selectively repulsed, which minimizes the area of illumination at the focal point and allows an enhancement of the resolution according to the intensity of the STED-pulse [2]. (iv) In expansion microscopy (ExM), the whole structure of interest is expanded using a polymer system and imaged using conventional fluorescence microscopy (FM) [6]. However, FM only visualizes fluorescent labels but the underlying cellular structures remain in the dark. The great advantage of electron microscopy (EM) is the revelation of cellular ultrastructures, membrane shapes, and organelle architecture. Nevertheless, the ultrastructural analysis is restricted to grayscale images [7, 8]. Structures that have not yet been morphologically described or related similar structures are hard to distinguish [9]. Additionally, in most applications, biological samples for EM are in a fixed and dehydrated state. The restraints of the two separate imaging modalities can be overcome by using correlative light and electron microscopy (CLEM). CLEM is the combination of (light)/fluorescence microscopy and EM. Therefore, CLEM techniques incorporate the labelling power of fluorescence imaging and the ultrastructural information provided by electron microscopy into one system [10].

While the fluorescence microscopy has the capacity to mark the regions of interest, the electron microscopy provides high-resolution information down to the nano-scale and allows the identification of the underlying structures of the fluorescent labels. Some CLEM techniques have achieved an unprecedented precision (<100 nm) for the localization of fluorescent dyes at an ultrastructural level [9, 11].

There is a plethora of different protocols and procedures on how to combine light and electron microscopy for CLEM [12, 13]. The different CLEM methods can be classified depending on when the FM micrographs are recorded, i.e. before (pre-embedding) or after the sample preparation (post-embedding) for EM. If FM is performed before embedding, there is a short time delay until the samples are fixed [14]. The main drawback of pre-embedding CLEM is that in the time between FM and EM measurements the observed structures may change due to processes and movements within the living cell, or may be altered by the subsequent EM-required embedding steps [15]. Post-embedding CLEM can be either performed on the entire embedded block using confocal microscopy or on sections suitable for EM. It has been shown that synthetic fluorophores maintain their fluorescence better in the presence of uranyl acetate than in cells or tissues which were treated with OsO_4 [16]. Compared to pre-embedding CLEM, FM imaging of sections is much more difficult because some fluorescence is always lost and the embedding resin can show some autofluorescence (i.e. Epon). However, the main advantage of post-embedding imaging is that during FM and EM the sample is not further manipulated and thus, the region of interest can be re-localized [15]. In summary, the sample preparation procedure is the fundamental step to keep a stable fluorescence signal and at the same time not to destroy the ultrastructure of the samples [17].

During the last years, CLEM has gained popularity within the field of cancer research as it is an important tool to gain new insights into transient events of the disease process [18–20]. Doxorubicin, a cytostatic agent from the group of anthracycline antibiotics, is widely used as a chemotherapeutic agent for cancer treatment [21]. The effect of doxorubicin is based on its intercalation in the DNA and its poisonous effect on topoisomerase II. The most dangerous side effects of the drug include cardiotoxicity and nephrotoxicity [22, 23]. Recently, Yang et al. showed that doxorubicin induces double strand breaks preferentially around active promoters. They propose that intercalation of anthracyclines enhance nucleosome turnover in a torsion-based manner, which exposes promoter DNA and increases the probability of strand breaks [24]. The big advantage of doxorubicin is its fluorescent property, which can be used to track the cytostatic pathway and to study the release of doxorubicin from the cell. CLEM

is the perfect tool to precisely visualize the subcellular localization of doxorubicin and its effects on the ultrastructure of treated cells and tissues. Unfortunately, so far, there is no prediction about the efficacy of the drug, the development of possible resistances and the subcellular sequestration of the chemotherapy.

Here, we discuss the use of post-embedding CLEM for the visualization and subcellular localization of a chemotherapeutic (i.e. doxorubicin) after treatment of cells and tumor tissue. For the first time, we apply this CLEM method on a tumor grown in the *in vivo* chorioallantoic membrane (CAM) model. The innovative CLEM technique focuses on the preservation of the fluorescence ability of doxorubicin throughout the preparation and imaging methodology in order to precisely localize the dye on electron micrographs.

2. Methods

2.1. Cell culture

MDCK II (Madin-Darby Canine Kidney) obtained from R. Thünauer, Albert-Ludwigs-Universität Freiburg, were grown in DMEM high glucose (Sigma-Aldrich, Taufkirchen, Germany) containing 5% FCS (BioWest, Nuaillé, France), at $37°C$ and $5\% CO_2$. The cultures were sub-cultured twice per week. Cells were densely grown in culture dishes and then treated for 30 min with 2 mg/ml DOXO-cell® (Stada Arzneimittel AG, Bad Vilbel, Germany). Afterwards the cells were washed twice with PBS and harvested with a cell scraper. Subsequently, cells were centrifuged for 5 min at 300 g and prepared for fluorescence and electron microscopy.

Alveolar rhabdomyosarcoma (ARMS) cells with a PAX3-FOXO1 translocation (RH 30) (from DSMZ (German Collection of Microorganisms and Cell Cultures GmbH, Braunschweig, Germany)) were cultivated in RPMI medium (Sigma-Aldrich, Taufkirchen, Germany) containing 10% FCS at $37°C$ and $5\% CO_2$ and passaged twice per week. For tumor inoculation, cells were harvested and counted in a Neubauer counting chamber. For the work with the human cell line, no approval from an Ethics Committee was required.

2.2. Tumors on the chorioallantoic membrane (CAM) model

The CAM assay was performed as described elsewhere [25, 26]. In brief, fertilized eggs were incubated for four days in a ProCon egg incubator (Grumbach, Asslar, Germany) at $37.8°C$ and 63% humidity. The whole procedure of the CAM model is shown in Fig. 3A. A window was cut into the eggshell to make the CAM accessible and was sealed with tape again for further incubation of the eggs. On the ninth day, 1×10^6 of the human ARMS cells (RH 30) mixed with Corning® Matrigel® (Fisher Scientific GmbH, Schwerte, Germany) in a 1:2 ratio were placed in a plastic ring, which was removed after 24 h, on the CAM. To investigate grown tumors *in ovo* and *ex ovo* the digital VHX-5000 microscope was used (Keyence, Neu-Isenburg, Germany) (Fig. 3B, C). On day 17, 500 µl DOXO-cell® 0.2 mg/ml were injected into a vein of the chorion (Fig. 3D, E). After 24 h, the tumors were explanted. Fluorescence signal of the explanted tumors was analyzed by FM (Fig. 4A, B). Tumor samples with positive fluorescence signal were prepared and fixed for CLEM as described below.

2.3. Sample preparation

MDCK II cells and tumors were fixed with a solution containing 1% glutaraldehyde, 4% paraformaldehyde and 2 mM $CaCl_2$ in 0.1 M sodium cacodylate buffer (pH 7.4) for 30 min at room

temperature and for four days at 4°C, respectively. After three washes with 0.1 M sodium cacodylate buffer (pH 7.4), samples were postfixed for 30 min with 0.1% osmium tetroxide in 0.1 M sodium cacodylate buffer. Thereafter, the specimens were washed five times with 0.1 M sodium cacodylate buffer and five times with ddH$_2$O and subsequently dehydrated in graded series of ethanol (20%, 50%, 70%, 90%, 100%) each for 5 min at 4°C and afterwards for 10 min with acetone at 4°C. Then, the samples were infiltrated for 30 min with a 1:1 mixture of Epon and acetone at 4°C, 2 h in Epon at 30°C and finally polymerized at 60°C for 48 h. Ultrathin sections of 90 nm were cut with a diamond knife (Diatome; Nidau, CH) on an ultramicrotome EM UC7 (Leica GmbH, Wetzlar, Germany). Sections were collected onto 200 mesh carbon-coated finder grids (Plano GmbH, Wetzlar, Germany). Grids with sections were analyzed by FM.

2.4. Fluorescence microscopy (FM) and imaging

The EM grid was placed on a 20 µl drop of ddH$_2$O on a microscope slide and, after adding a second drop of ddH$_2$O, closed with a high precision cover slip. After adding a drop of immersion oil, EM grids were faced towards the objective during imaging. All images were taken on a Axiovert 200 mot inverted microscope (Zeiss, Oberkochen, Germany) equipped with a Fluar 100 × 1.3 oil objective (Zeiss, Oberkochen, Germany), a sCMOS-camera (PCO AG, Kehlheim, Germany) and electronic shutters, at room temperature. The microscope was controlled by VisiView version 4.1.0.4 (Visitron Systems GmbH, Puchheim, Germany). Images were acquired using an external light source HXP-120 (Visitron Systems GmbH, Puchheim, Germany), an ET 560/40 nm narrow band excitation filter and an ET630/75 emission filter. Z-stacks of 19 layers (0.45 nm each) were taken at standard exposure time and thereafter processed with ImageJ (National Institutes of Health, Bethesda, USA). After imaging, the grids were removed from microscope slides and dried for use in EM.

2.5. Transmission electron microscopy (TEM)

Sections were contrasted using 1% uranyl acetate in ddH$_2$O for 30 min and examined at 80 kV using an EM 902 transmission electron microscope (Zeiss, Oberkochen, Germany). Electron micrographs were recorded digitally using a CCD camera together with the software Image SP (2048 × 2048 pixels; TRS, Moorenweis, Germany).

2.6. Dataset processing by easy cell-correlative light to electron microscopy (eC-CLEM)

The free open-source software eC-CLEM (a plugin for the image analysis software ICY) [27, 28] was used to generate precise virtual overlays of FM and TEM datasets. TEM and FM images were aligned and correlated by computing similarities. Overlay images were saved.

3. Results

3.1. CLEM of MDCK II cells treated with doxorubicin

Cultured MDCK II cells were treated with 2 mg/ml doxorubicin for 30 min and afterwards embedded for microscopy (Fig. 1). Initially, inverted fluorescence light microscopy was used to see the localization of doxorubicin (Fig. 2A). Afterwards, the same sections were analyzed by transmission electron microscopy (TEM) (Fig. 2B). Finally, the obtained information at the different length scales of both techniques were correlated using the software package eC-CLEM/ICY, which enables the
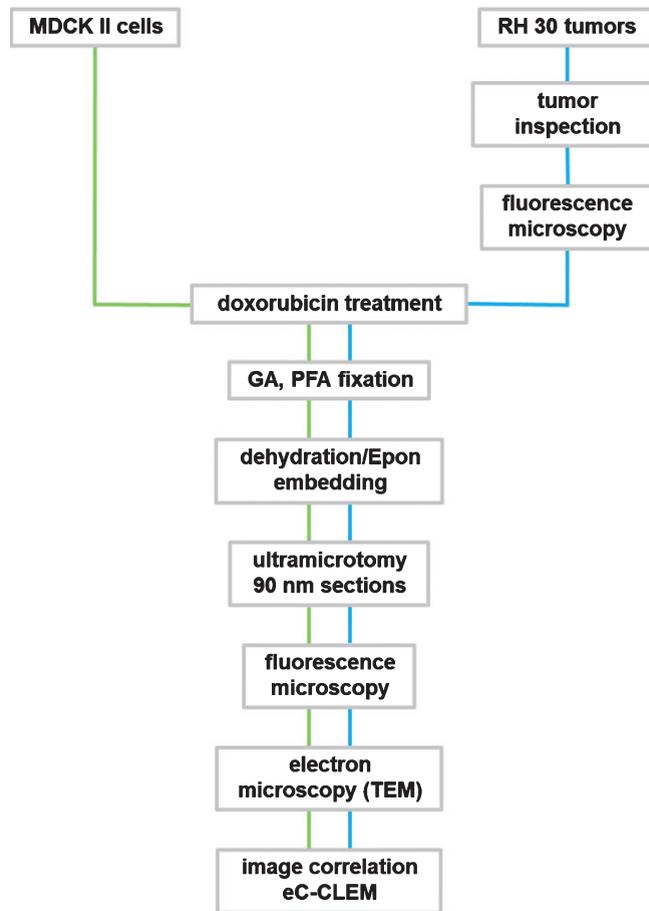
Fig. 1. Flowchart for CLEM methodology of doxorubicin treated cell and tumor samples. GA: glutaraldehyde; PFA: paraformaldehyde.

precise overlay of both datasets of structural information (Fig. 2C). The correlation accuracy achieved was about 60 nm. After 30 min exposure to doxorubicin, the kidney epithelial cells showed a clear localization of the chemotherapeutic in the nucleus, which correlated with electron-dense regions (heterochromatin) (Fig. 2A, C). TEM/CLEM showed increased membrane blebbings in the cytoplasm and increased formation of microvilli (Fig. 2B, C).

3.2. CLEM of doxorubicin treated tumors grown on CAM

To investigate whether the CLEM method is also suitable to study the localization of doxorubicin in tumors in the *in vivo* CAM model, we used RH 30 cells to grow tumors on the CAM. The doxorubicin-injected tumors were explanted 24 h after doxorubicin injection from the CAM and checked for a positive fluorescence signal. Compared to the application of doxorubicin in cells (exposure to the drug for 30 min), doxorubicin needs to be transported into the tumor tissue on the CAM via the blood circulation. Tumors with a promising fluorescence signal were chosen for embedding (Fig. 4A). Tumors with low or no fluorescence were not further processed (Fig. 4B). The analyzed tumors show a clear staining of the cell nuclei, and the fluorescence of doxorubicin correlates with electron-dense areas of the cell nuclei (Fig. 4C, D, E). The TEM images show that doxorubicin treatment leads to an enormous stress situation of the cell with an increased formation of membrane blebbings.
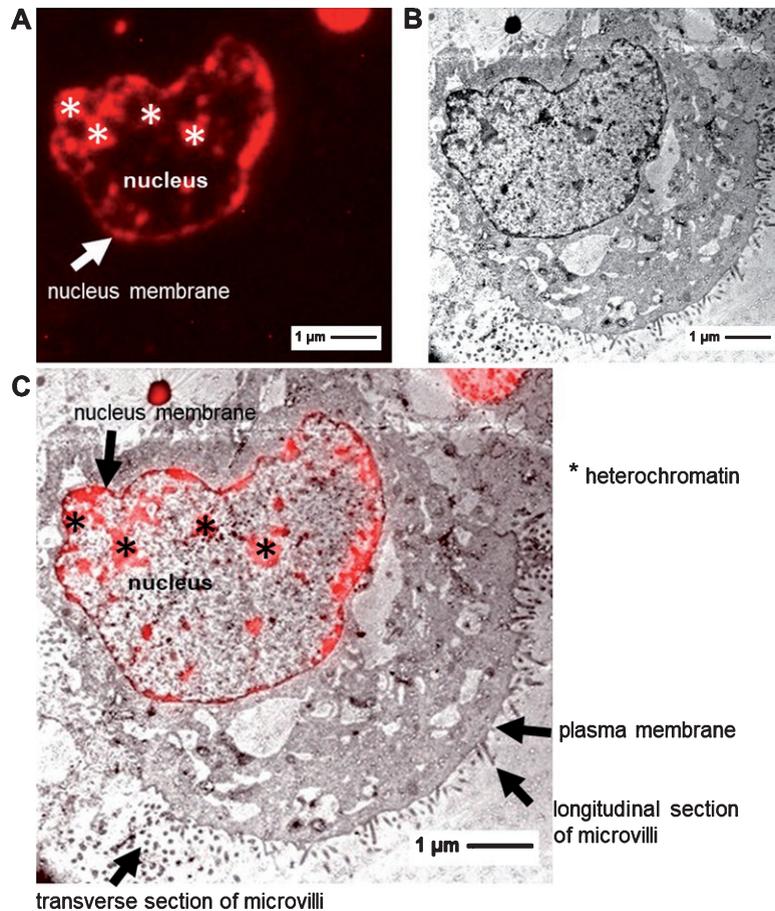
Fig. 2. Images of doxorubicin treated MDCK II cells. A: FM image B: TEM image C: CLEM image.

4. Discussion

In the present work, we established a CLEM method that is applicable to a wide field of cancer research. An advantage of many chemotherapeutic drugs (i.e. doxorubicin) is their autofluorescence, which makes them particularly compatible with CLEM. Therefore, neither additional fluorescence labeling techniques are required nor fluorescent proteins are needed. We were able to show that the fluorescent property of the chemotherapeutic substance doxorubicin behaves completely differently from those of fluorescent proteins during sample preparation for EM. The fluorescence ability of doxorubicin proved to be quite resistant to quenching during the fixation, dehydration and embedding procedure or to photobleaching during FM. Epon embedding provides the best structure preservation for electron microscopy [29, 30]. In many cases, glutaraldehyde fixation, room-temperature dehydration, and also Epon embedding resulted in severe losses of fluorescence. As our investigations show that the fluorescence ability of doxorubicin withstands our preparation protocol, we have set up a post-embedding CLEM approach, accordingly, with success. Furthermore, the time needed for the embedding protocol could be substantially reduced as doxorubicin requires no additional treatment steps for fluorescence preservation. We describe a promising new method to visualize the pattern of doxorubicin in cells and for the first time for an *in vivo* tumor grown on CAM. This established method precisely localizes doxorubicin using electron microscopic resolution.
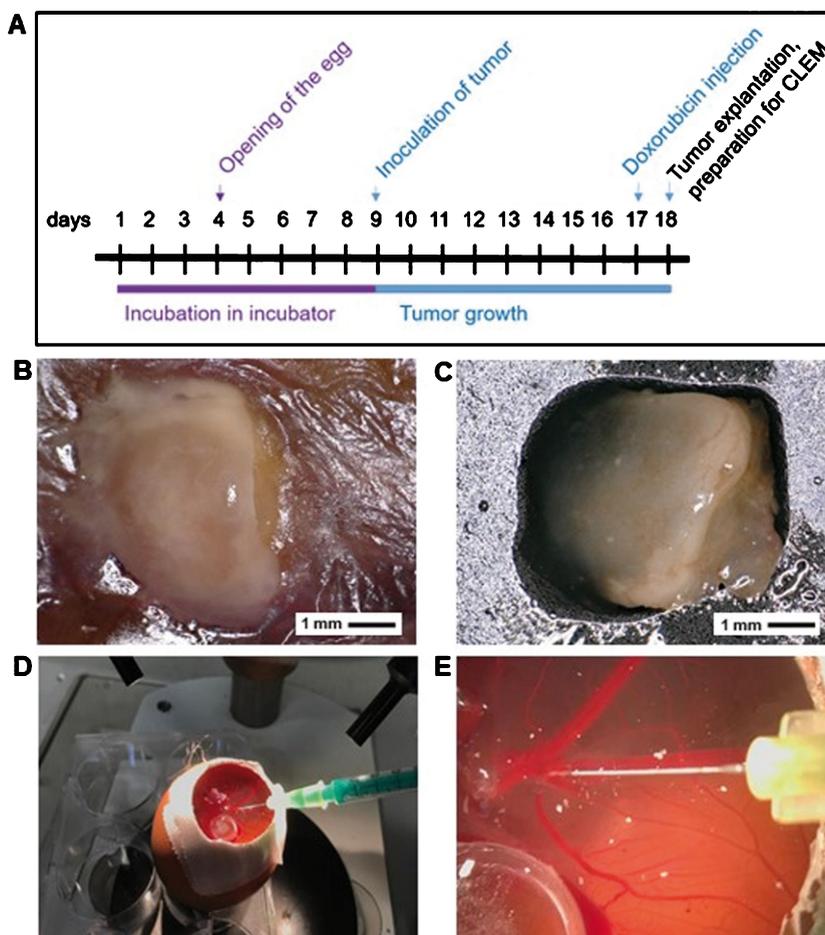
Fig. 3. Tumor growth on CAM and treatment with doxorubicin. A: Time schedule of CAM assay. B, C: *In ovo* tumor growth (B) and *ex ovo* tumor (C) of RH 30 cells. D, E: Intravenous injection of doxorubicin.

The correlation accuracy achieved in our CLEM experiments was about 60 nm. In principal, an accuracy of <500 nm is called "high accurate" [12]. Our correlation accuracy is also comparable to publications from Kukulski et al. [9] or Schorb et al. [31] showing an accuracy of about 100 nm. Using fluorescent fiducial markers Schellenberg et al. [11] also achieved a correlation accuracy of about 60 nm in their CLEM studies. To reach a significant higher overall accuracy (less than 50 nm), the use of fluorescent fiducial markers is needed [32]. For our study, the accuracy of 60 nm is sufficient. If a higher accuracy will be required to investigate the localization of other drugs by CLEM, e.g. TetraSpecks with a diameter of 50 nm (Thermo Fisher Scientific) could be easily applied to the resin sections as described by Schorb et al. to complement our CLEM method [31].

One possible perspective for our CLEM technique is the use for the structural and functional detection of drugs/medical therapies. Drugs, coupled to fluorescence that attack (i) the nucleus (e.g. doxorubicin), or (ii) organelles in the cytosol (e.g. sorafenib), or (iii) surface structures of the cell membrane (e.g. rituximab), or (iv) are bound to/absorbed by exosomes/extracellular vesicles may be detected and localized by CLEM: (i) Drugs that intercalate in the DNA and either have autofluorescence (e.g. doxorubicin) or carry a fluorescent label. (ii) Drugs that attack organelles in the cytosol. These include proteasome inhibitors such as the cytostatic bortezomib, substances that inhibit tubulin growth, such as vincaalkaloids (vincristin, vinblastin) and tyrosine kinase-inhibitors that interfere with intracellular
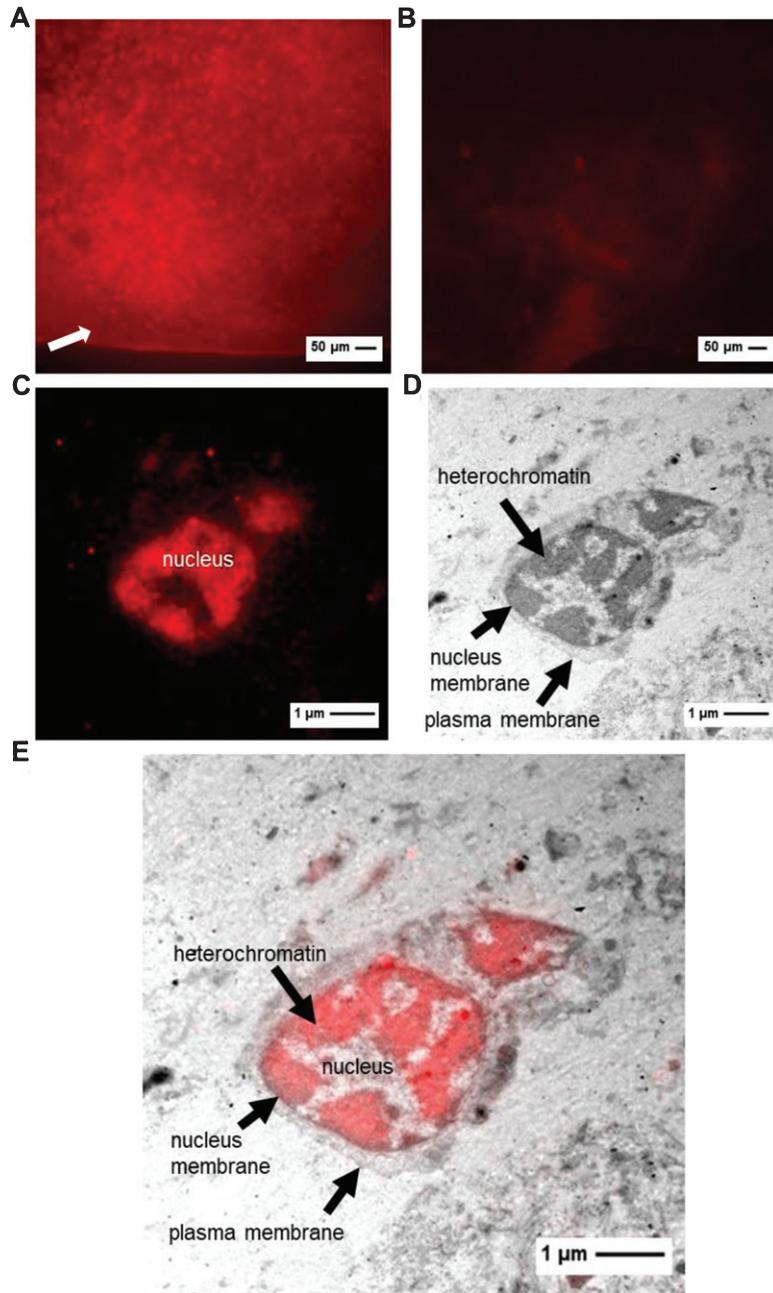
Fig. 4. A, B: FM of tumor with high (A) or low fluorescence (B) before embedding (exposure time 40 ms). Arrow indicates chorion membrane. C–E: images of RH 30 tumor (C: FM image D: TEM image E: CLEM image).

signaling pathways, such as sorafenib, dasatinib and imatinib. The latter is usually detected using radiolabeled C^{14} [33]. The results generated with our CLEM technique let assume that this method is an alternative and safer approach to detect imatinib. (iii) Drugs/antibodies that recognize therapeutically relevant surface structures of the cell membrane. For example, the chimeric antibody rituximab recognizes CD20 and bevacizumab acts as an angiogenesis inhibitor due to VEGF blockage. (iv) Finally, membrane blebbings including exosomes and extracellular vesicles (50–100 nm) can be detected by means of CLEM. Chemotherapeutics, in particular anthracyclines, enter tumor cells and subsequently

the nucleus. However, the tumor cells rapidly sequester the active component (e.g. doxorubicin) imme-diately into subcellular compartments and transport it - concentrated in exosomes - outside of the cell [34]. Tumor exosomes, which bind drugs, act as a "protective shield" around the tumors making the drug locally ineffective. On the surface, exosomes carry proteins like the therapeutic target CD20 bind-ing the anti-CD20 chimeric antibody rituximab and inducing a resistance mechanism of the tumor. Furthermore, complement-regulating proteins like CD46, 55 and 59 down-regulate parts of the com-plement system leaving exosomes unscathed and depleting the complement protecting the tumor [35]. Moreover, it has been shown that exosomes express immunomodulatory proteins (e.g. TRAIL, Fas ligand) on their surface [36]. These can have immuno-suppressive effects in the tumor niche and in the pre-metastatic niche [37]. Simon et al. demonstrated that glioblastoma elude anti-angiogenic therapy with bevacizumab by internalizing the antibody and releasing more extracellular vesicles carrying the antibody [38].

In summary, CLEM is a promising method to functionally and structurally detect fluorescing drugs (e.g. doxorubicin, paclitaxel, bleomycin) [39] whose target structures are in the nucleus, in the cytosol or on the membrane surface.

5. Conclusion

Our CLEM method represents an innovative method of visualization for the autofluorescent cytostatic drug doxorubicin. Accurate representation of subcellular architectures and morphology is possible due to high-resolution electron microscopy. Perspectively, this powerful imaging method may be used to study the effect of fluorescent drugs in patient material and to develop promising prevention and treatment strategies at the cellular level.

Conflict of interest

The authors declare no competing interests.

Acknowledgments

We thank Lucia Denk and Dipl. Biol. Manfred Depner for their excellent technical support.

References

[1] Schermelleh L, Heintzmann R, Leonhardt H. A guide to super-resolution fluorescence microscopy. J Cell Biol. 2010;190(2):165-75. doi:10.1083/jcb.201002018

[2] Hell SW, Wichmann J. Breaking the diffraction resolution limit by stimulated emission: Stimulated-emission-depletion fluorescence microscopy. Opt Lett. 1994;19(11):780-2. doi:10.1364/ol.19.000780

[3] Betzig E, Patterson GH, Sougrat R, Lindwasser OW, Olenych S, Bonifacino JS, et al. Imaging intracellular fluorescent proteins at nanometer resolution. Science. 2006;313(5793):1642-5. doi:10.1126/science.1127344

[4] Suleiman H, Zhang L, Roth R, Heuser JE, Miner JH, Shaw AS, et al. Nanoscale protein architecture of the kidney glomerular basement membrane. Elife. 2013;2:e01149. doi:10.7554/eLife.01149

[5] Pullman JM, Nylk J, Campbell EC, Gunn-Moore FJ, Prystowsky MB, Dholakia K. Visualization of podocyte sub-structure with structured illumination microscopy (SIM): A new approach to nephrotic disease. Biomed Opt Express. 2016;7(2):302-11. doi:10.1364/BOE.7.000302

[6] Wang Y, Yu Z, Cahoon CK, Parmely T, Thomas N, Unruh JR, et al. Combined expansion microscopy with structured illumination microscopy for analyzing protein complexes. Nat Protoc. 2018;13(8):1869-95. doi:10.1038/s41596-018-0023-8

[7] Porter KR, Claude A, Fullam EF. A study of tissue culture cells by electron microscopy methods and preliminary observations. J Exp Med. 1945;81(3):233-46. doi:10.1084/jem.81.3.233

[8] Masters BR, editor. Encyclopedia of Life Sciences (ELS): History of the ElectronMicroscope in Cell Biology. Chichester: John Wiley & Sons, Ltd; 2009.

[9] Kukulski W, Schorb M, Welsch S, Picco A, Kaksonen M, Briggs JAG. Correlated fluorescence and 3D electron microscopy with high sensitivity and spatial precision. J Cell Biol. 2011;192(1):111-9. doi:10.1083/jcb.201009037

[10] Biel SS, Kawaschinki K, Wittern K-P, Hintze U, Wepf R. From tissue to cellular ultrastructure: Closing the gap between micro- and nanostructural imaging. J Microscopy 2003;212:91-99.

[11] Schellenberger P, Kaufmann R, Siebert CA, Hagen C, Wodrich H, Grunewald K. High-precision correlative fluorescence and electron cryo microscopy using two independent alignment markers. Ultramicroscopy. 2014;143:41-51. doi:10.1016/j.ultramic.2013.10.011

[12] Boer P de, Hoogenboom JP, Giepmans BNG. Correlated light and electron microscopy: Ultrastructure lights up!. Nat Methods. 2015;12(6):503-13. doi:10.1038/nmeth.3400

[13] Timmermans FJ, Otto C. Contributed review: Review of integrated correlative light and electron microscopy. Rev Sci Instrum. 2015;86(1):11501. doi:10.1063/1.4905434

[14] Verkade P. Moving EM: The Rapid Transfer System as a new tool for correlative light and electron microscopy and high throughput for high-pressure freezing. J Microsc. 2008;230(Pt 2):317-28. doi:10.1111/j.1365-2818.2008.01989.x

[15] Bykov YS, Cortese M, Briggs JAG, Bartenschlager R. Correlative light and electron microscopy methods for the study of virus-cell interactions. FEBS Lett. 2016;590(13):1877-95. doi:10.1002/1873-3468.12153

[16] Perkovic M, Kunz M, Endesfelder U, Bunse S, Wigge C, Yu Z, et al. Correlative light- and electron microscopy with chemical tags. J Struct Biol. 2014;186(2):205-13. doi:10.1016/j.jsb.2014.03.018

[17] Kishi-Itakura C, Buss F. The Use of Correlative Light-Electron Microscopy (CLEM) to Study PINK1/Parkin-Mediated Mitophagy. Methods Mol Biol. 2018;1759:29-39. doi:10.1007/7651_2017_8

[18] Voorneveld PW, Kodach LL, Jacobs RJ, Liv N, Zonnevylle AC, Hoogenboom JP, et al. Loss of SMAD4 alters BMP signaling to promote colorectal cancer cell metastasis via activation of Rho and ROCK. Gastroenterology. 2014;147(1):196-208.e13. doi:10.1053/j.gastro.2014.03.052

[19] Karreman MA, Mercier L, Schieber NL, Solecki G, Allio G, Winkler F, et al. Fast and precise targeting of single tumor cells *in vivo* by multimodal correlative microscopy. J Cell Sci. 2016;129(2):444-56. doi:10.1242/jcs.181842

[20] Othman BA, Greenwood C, Abuelela AF, Bharath AA, Chen S, Theodorou I, et al. Correlative Light-Electron Microscopy Shows RGD-Targeted ZnO Nanoparticles Dissolve in the Intracellular Environment of Triple Negative Breast Cancer Cells and Cause Apoptosis with Intratumor Heterogeneity. Adv Healthc Mater. 2016;5(11):1310-25. doi:10.1002/adhm.201501012

[21] Weiss RB. The anthracyclines: Will we ever find a better doxorubicin? Semin Oncol. 1992;19(6):670-86.

[22] Lahoti TS, Patel D, Thekkemadom V, Beckett R, Ray SD. Doxorubicin-induced *in vivo* nephrotoxicity involves oxidative stress-mediated multiple pro- and anti-apoptotic signaling pathways. Curr Neurovasc Res. 2012;9(4):282-95.

[23] Chatterjee K, Zhang J, Honbo N, Karliner JS. Doxorubicin cardiomyopathy, Cardiology. 2010;115(2):155-62. doi:10.1159/000265166

[24] Yang F, Kemp CJ, Henikoff S. Anthracyclines induce double-strand DNA breaks at active gene promoters. Mutat Res. 2015;773:9-15. doi:10.1016/j.mrfmmm.2015.01.007

[25] Kauffmann P, Troeltzsch M, Cordesmeyer R, Heidekrueger PI, Schliephake H, Canis M, et al. Presentation of a variation of the chorioallantoic membrane set up as a potential model for individual therapy for squamous cell carcinoma of the oropharynx, Clin Hemorheol Microcirc. 2017;67(3-4):453-7. doi:10.3233/CH-179226

[26] Kauffmann P, Troeltzsch M, Brockmeyer P, Bohnenberger H, Heidekruger PI, Manzke M, et al. First experience of chick chorioallantoic membrane (CAM) assay in the clinical work flow with oral squamous cell carcinoma patients. Clin Hemorheol Microcirc. 2018;70(4):487-94. doi:10.3233/CH-189315

[27] Paul-Gilloteaux P, Heiligenstein X, Belle M, Domart M-C, Larijani B, Collinson L, et al. eC-CLEM: Flexible multidimensional registration software for correlative microscopies. Nat Methods. 2017;14(2):102-3. doi:10.1038/nmeth.4170

[28] Chaumont F de, Dallongeville S, Chenouard N, Herve N, Pop S, Provoost T, et al. Icy: An open bioimage informatics platform for extended reproducible research. Nat Methods. 2012;9(7):690-6. doi:10.1038/nmeth.2075

[29] del Castillo P, Molero ML, Ferrer JM, Stockert JC. Autofluorescence and induced fluorescence in Epon embedded tissue sections, Histochemistry. 1986;85(5):439-40.

[30] Craig EL, Frajola WJ, Greider MH. An embedding technique for electron microscopy using EPON 812, J Cell Biol. 1962;12:190-4. doi:10.1083/jcb.12.1.190

[31] Schorb M, Gaechter L, Avinoam O, Sieckmann F, Clarke M, Bebeacua C, et al. New hardware and workflows for semi-automated correlative cryo-fluorescence and cryo-electron microscopy/tomography. J Struct Biol. 2017;197(2):83-93. doi:10.1016/j.jsb.2016.06.020

[32] Mohammadian S, Fokkema J, Agronskaia AV, Liv N, Heus C de, van Donselaar E, et al. High accuracy, fiducial marker-based image registration of correlative microscopy images. Sci Rep. 2019;9(1):3211. doi:10.1038/s41598-019-40098-4

[33] Chapuy B, Panse M, Radunski U, Koch R, Wenzel D, Inagaki N, et al. ABC transporter A3 facilitates lysosomal sequestration of imatinib and modulates susceptibility of chronic myeloid leukemia cell lines to this drug. Haematologica. 2009;94(11):1528-36. doi:10.3324/haematol.2009.008631

[34] Koch R, Aung T, Vogel D, Chapuy B, Wenzel D, Becker S, et al. Nuclear Trapping through Inhibition of Exosomal Export by Indomethacin Increases Cytostatic Efficacy of Doxorubicin and Pixantrone. Clin Cancer Res. 2016;22(2):395-404. doi:10.1158/1078-0432.CCR-15-0577

[35] Aung T, Chapuy B, Vogel D, Wenzel D, Oppermann M, Lahmann M, et al. Exosomal evasion of humoral immunotherapy in aggressive B-cell lymphoma modulated by ATP-binding cassette transporter A3. Proc Natl Acad Sci U S A. 2011;108(37):15336-41. doi:10.1073/pnas.1102855108

[36] Stenqvist A-C, Nagaeva O, Baranov V, Mincheva-Nilsson L. Exosomes secreted by human placenta carry functional Fas ligand and TRAIL molecules and convey apoptosis in activated immune cells, suggesting exosome-mediated immune privilege of the fetus. J Immunol. 2013;191(11):5515-23. doi:10.4049/jimmunol.1301885

[37] Guo Y, Ji X, Liu J, Fan D, Zhou Q, Chen C, et al. Effects of exosomes on pre-metastatic niche formation in tumors. Mol Cancer. 2019;18(1):39. doi:10.1186/s12943-019-0995-1

[38] Simon T, Pinioti S, Schellenberger P, Rajeeve V, Wendler F, Cutillas PR, et al. Shedding of bevacizumab in tumour cells-derived extracellular vesicles as a new therapeutic escape mechanism in glioblastoma. Mol Cancer. 2018;17(1):132. doi:10.1186/s12943-018-0878-x

[39] Motlagh NSH, Parvin P, Ghasemi F, Atyabi F. Fluorescence properties of several chemotherapy drugs: Doxorubicin, paclitaxel and bleomycin. Biomed Opt Express. 2016;7(6):2400-6. doi:10.1364/BOE.7.002400